land

MDPI

Article

Assessment of Soil Erosion from an Ungauged Small Watershed and Its Effect on Lake Ulansuhai, China

Zhuangzhuang Zhang [1] and Ruihong Yu [1,2,3,*]

[1] Inner Mongolia Key Laboratory of River and Lake Ecology, School of Ecology and Environment, Inner Mongolia University, Hohhot 010021, China
[2] Key Laboratory of Ecology and Resources Use of the Mongolian Plateau of Ministry of Education, Hohhot 010021, China
[3] Autonomous Region Collaborative Innovation Center for Integrated Management of Water Resources and Water Environment in the Inner Mongolia Reaches of the Yellow River, Hohhot 010018, China
* Correspondence: rhyu@imu.edu.cn; Tel.: +86-471-4991729

Abstract: Lake Ulansuhai, one of the main water sources for semi-arid areas of China, has a local deposit caused by soil erosion during past decades. However, a lack of monitor stations prevents better estimation of soil erosion levels. Therefore, we try to estimate soil erosion in the Huangtuyaozi (HTYZ) watershed, an ungauged small watershed of the lake's eastern watershed, by using the revised universal soil loss equation (RUSLE) model and multi-source remote sensing data, and analyze its key drivers and effect on the lake siltation. The result showed that the soil erosion rate in the HTYZ watershed ranged from 0 to 129.893 t ha^{-1} yr^{-1} with an average of 6.45 t ha^{-1} yr^{-1} during 1986–2015. In particular, 80.06% of the area was less than 10 t ha^{-1} yr^{-1}, and just 0.06% was over 50 t ha^{-1} yr^{-1}, mainly in the mountain area, the southern part of the HTYZ watershed. Moreover, rainfall erosivity factor is the key factor, and rainfall during flood season plays a key role in soil erosion. Due to the soil erosion of HTYZ, siltation in Lake Ulansuhai reached 223.83 ha, with the annual siltation area increasing at a rate of 7.46 ha/yr. The results could provide a reference for estimating soil erosion of ungauged small watershed in semi-arid areas.

Keywords: soil erosion; RUSLE; ungauged small watershed; Lake Ulansuhai; semi-arid areas

Citation: Zhang, Z.; Yu, R. Assessment of Soil Erosion from an Ungauged Small Watershed and Its Effect on Lake Ulansuhai, China. *Land* **2023**, *12*, 440. https://doi.org/10.3390/land12020440

Academic Editor: Wojciech Zgłobicki

Received: 23 December 2022
Revised: 2 February 2023
Accepted: 4 February 2023
Published: 8 February 2023

1. Introduction

Soil erosion is one of the serious problems in many countries and has received much attention in recent years [1]. Globally, soil erosion has affected a 1094 Mha land area, including 751 Mha of extensive erosion [2]. In recent years, soil erosion has become one of the major threats to the ecology and environment of arid regions due to climate change and anthropogenic activities. Soil erosion has led to siltation of lakes, decline of soil fertility, and a series of serious environmental problems [3–5]. In a semi-arid area, freshwater is a vital resource as it is not only important for human activities, but also plays an important function in regulating the ecological environment. However, lakes are commonly affected by soil erosion in this area in recent years because of the fragile ecology, and the biodiversity has also decreased [6,7]. In semi-arid regions, soil erosion depends on various natural factors such as rainfall, soil properties, vegetation and topography. However, the scarcity of gauged stations and the large areas in arid regions made it difficult to accurately estimate soil erosion. Thus, it is necessary to accurately estimate the severity of soil erosion in order to protect the fragile lake ecosystems in arid regions.

In current studies, one of the most complex problems is obtaining a more accurate estimate of the soil erosion for a watershed scale. Monitoring soil loss in situ based on actual measurements of field plots is the most valid method [8,9]. However, systematic field measurements are very costly as they require significant human and technological resources. With the development of soil erosion studies, various soil erosion models have

been applied to assess soil erosion, because models could provide quantitative estimation based on different scenarios. Currently, soil erosion is mainly divided into two types, including physically-based models and empirical models. The physically-based soil erosion models, such as the Water Erosion Prediction Project (WEPP) model [10] and the European Soil Erosion Model (EUROSEM) [11], can provide accurate estimation for soil erosion; however, the lack of numerous parameters (i.e., hydrology, soil mechanics parameters, etc.) is a major obstacle for the application of such models. Thus, many previous studies selected empirical models, such as the universal soil loss equation (USLE) [12], the revised universal soil loss equation (RUSLE) [13], and Soil and Water Assessment Tool (SWAT) [14], to estimate soil erosion because these models have simple and robust features. USLE and RUSLE are widely used models because they are robust, parameter data are readily available and analyzed, and many researchers have modified it to apply to local regions. Previous studies found that the application of USLE is limited because of land use types and topography (croplands and gently sloping topography). The RUSLE has been accepted globally for its applicability to a wide range of land use types and topography (croplands, forest, grassland, gentle to steep slopes, etc.). With the development of remote sensing (RS) and geographic information system (GIS) technologies, the RUSLE model combined with RS and GIS could accurately estimate soil erosion in various regions. Markose et al. [15] and Thomas et al. [16] estimated the soil erosion in a tropical basin in India using RUSLE and GIS, and achieved good results. Du et al. [17] and Djoukbala et al. [18] also estimated the soil erosion in a large-scale area (>10,000 km^2) of a semi-arid region using RUSLE and GIS. However, few studies have focused on the application of RUSLE to estimate soil erosion in ungauged small watersheds in semi-arid regions.

Currently, various RS data were applied to soil erosion, and they have solved the problem of soil erosion estimation in large regions. Landsat satellite data and digital elevation model (DEM) data are usually used for the dataset to calculate model parameters. However, while precipitation data can provide the key parameter in the model because to calculate rainfall erosivity, previous studies have usually used different satellites such as the Tropical Rainfall Measuring Mission (TRMM) satellite, which cannot obtain long time series data. Furthermore, various databases were built to estimate rainfall erosivity on regional and global scales. Bezak et al. [19] reconstruct rainfall erosivity and trends across Europe during 1961–2018 based on the REDES database. As a high-precision global dataset, the Climatologies at high resolution for the earth's land surface areas (CHELSA) dataset has covered past decades, and it has been widely used in many fields. Moradi et al. [20] used CHELSA climate data to analyze plant functional diversity. Zuquim et al. [21] used CHELSA precipitation data to analyze the suitability of plant habitats in a tropical forest. Fang et al. [22] used CHELSA precipitation data to calculate the annual precipitation in a large area of an arid region. Kazamias et al. [23] used the CHELSA precipitation data to calculate rain erosivity over Greece. Thus, this study tries to use CHELSA precipitation data as the input data of the model in the small watershed of semi-arid region.

Overall, we test the following hypotheses: (1) CHELSA data with high accuracy could be used for an ungauged station in a small watershed in the semi-arid areas; (2) the spatial variation of soil erosion in the ungauged small watershed during a long time period could be satisfactorily estimated by combining the RUSLE model with multi-resource RS data; and (3) soil erosion during flood season is the main reason for the lake's local siltation. Huangtuyaozi (HTYZ) watershed, an ungauged small watershed east of Lake Ulansuhai, which is the largest shallow lake in the Yellow River basin, was selected as the study area. The aims of the present study were (1) combining the RUSLE model with RS and GIS technology to estimate the soil erosion level of HTYZ during the past 30 years; (2) analyzing the key factors of soil erosion in the HTYZ area; and (3) mapping the siltation area of Lake Ulansuhai during study period, and analyzing its potential drivers.

2. Materials and Methods

2.1. Study Area

The Huangtuyaozi (HTYZ) area is situated to the east of Lake Ulansuhai, Bayannur in Inner Mongolia, China. Geographically, HTYZ is located between 108°58′10″ and 109°28′36″ E longitude and 40°42′48″ and 40°56′19″ N latitude, and covers an area of 349.94 km^2 (Figure 1). The elevation of HTYZ ranges from 978 m to 2268 m above mean sea level. Moreover, the northern and central parts of HTYZ are dominated by plains, but the southern part is dominated by mountains. The slope ranges from 0 to 57.9 degrees with an average slope of about 11.8 degrees, and the contribution of flat (0–5%), moderate (5–25%), and steep (>25%) slopes cover 31.6%, 56.0%, and 12.4% of the area, respectively.

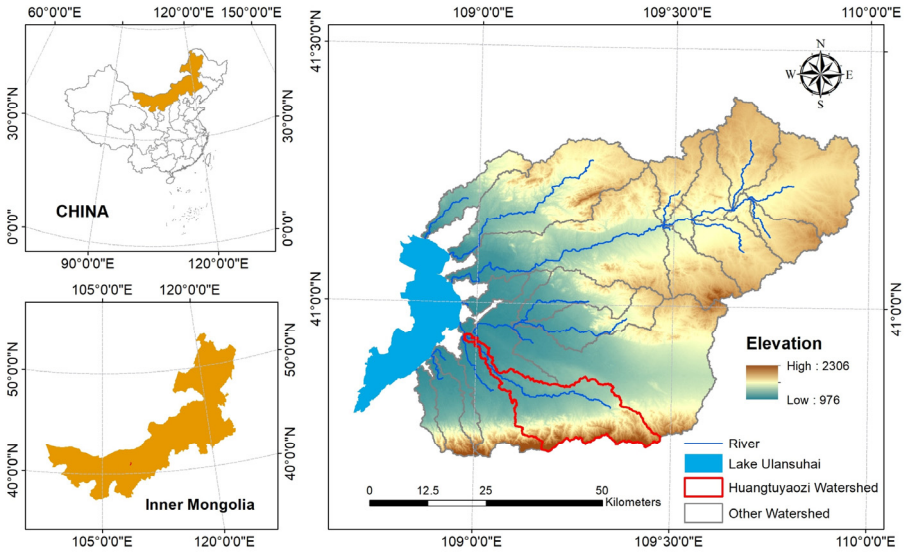

Figure 1. Location of the Huangtuyaozi (HTYZ) watershed and its relative position with Lake Ulansuhai, China.

The climate of HTYZ is a temperate continental climate with a rainy season from June to September, which often accounts for 73% of the annual precipitation. During 1986–2015, the mean annual precipitation of HTYZ ranged 204–360 mm [24]. The southern part of HTYZ is the rainfall center of the watershed with mean annual precipitation of >300 mm. The mean annual temperature in HTYZ is 6.6 °C with maximum temperatures occurring during July (24.6 °C) and minimum during January (−10.2 °C) [25].

The major soil type of HTYZ is *Haplic Kastanozems*, which is a common soil type in arid regions, covering 33.4% of HTYZ. The other common soil types are *Calcaric Cambisols* (23.65%) and *Cambic Arenosols* (23.21%), which are alluvial soils that are susceptible to erosion (Table S3). Grassland is the main land type of HTYZ (72.92%), of which low coverage grassland accounts for 4.25% of HTYZ, moderate coverage grassland accounts for 38.49% of HTYZ, and high coverage grassland accounts for 30.18% of the total area. Sand accounts for 12.18% of HTYZ, mainly closer to Lake Ulansuhai. The other land types include woodland (7.33%), shrub land (6.91%) and Bare land (0.66%) (2010 LUCC).

2.2. Estimation of RUSLE Parameters

Soil erosion models are useful in estimating spatial and temporal soil erosion loss. RULSE was selected to estimate the longtime annual soil erosion as the model is robust and parameter data is readily available and analyzed. The data of RUSLE is usually generated by remote sensing images (i.e., rainfall maps, soil property maps, etc.); thus, it is easily available through open-source databases. The calculations of RUSLE model factors are easily integrated into GIS software for easy processing and analysis.

The RUSLE model was used to calculate the mean annual soil loss (A) per unit area due to the erosivity of rain-runoff (R), erodibility of the soil (K), slope length/slope steepness (LS), cover management (C), and support practice (P) factors.

Mean annual soil loss (A) was computed using Equation (1), as per Wischmeier et al. [12] and Renard et al. [13]:

$$A = R \cdot K \cdot LS \cdot C \cdot P \quad (1)$$

where A is the computed average annual soil erosion (t ha^{-1} yr^{-1}), R is rainfall erosivity factor (MJ mm ha^{-1} mm^{-1}), K is soil erodibility factor (t ha^{-1} MJ^{-1} mm^{-1}), LS is slope length and slope steepness factor (dimensionless), C is the cover management factor (dimensionless), and P is the support practice factor (dimensionless).

The rainfall erosivity factor (R) is an important factor of soil erosion. It is defined as the product of total energy (E) and a maximum 30 min rainfall intensity (I_{30}), and requires at least 20 years of data. However, most regions cannot calculate R due to a lack of data. Thus, many simplified models were developed to replace E and I_{30}. In this study, the R factor was calculated using Equation (2), a widely used equation in arid regions proposed by Hurni [26]:

$$R = 0.55 \times P - 24.7 \quad (2)$$

where R is the rainfall erosivity factor (MJ mm ha^{-1} mm^{-1}) and P is the annual rainfall (mm).

In this study, Climatologies at high resolution for the earth's land surface areas (CHELSA) monthly precipitation (http://chelsa-climate.org/, accessed on 1 December 2022) was used to obtain annual rainfall data for HTYZ. CHELSA is a high resolution (30 arc sec) climate dataset for the earth land surface areas, currently hosted by the Swiss Federal Institute for Forest, Snow and Landscape Research WSL, and is based on a quasi-mechanistic statistical downscaling of the ERA interim global circulation model for precipitation [27]. In this study, 30 years of CHELSA precipitation data (1986–2015) were selected to calculate the R factor after re-sampling to 30 m in ArcGIS 10.2 software.

The soil erodibility factor (K) represents the inherent susceptibility of soil erosion, reflects the rate of soil loss per rainfall erosivity index, and is strongly related to the soil physical properties [28]. All K factor models require soil texture, soil organic matter, and percentage of sand, silt, and clay in the soil [29].

K factor was calculated using Equation (3), given by Neitsch et al. [30].

$$K = f_{csand} \cdot f_{cl-ci} \cdot f_{orgc} \cdot f_{hisand} \quad (3)$$

where f_{csand} is a factor that gives low K factor for soil with high coarse-sand contents and high values for soils with little sand. $f_{cl\text{-}si}$ is a factor that gives a low K factor for soils with high clay to silt ratios, f_{orgc} is a factor that reduces K for soils with high organic carbon content, and f_{hisand} is a factor that reduces K for soils with extremely high sand content. The factors were computed as follows:

$$f_{csand} = 0.2 + 0.3 \cdot \exp[-0.256 \cdot m_s \cdot (\frac{1 - m_{silt}}{100})] \quad (4)$$

$$f_{cl-si} = \frac{m_{silt}}{m_c + m_{silt}} \quad (5)$$

$$f_{orgc} = 1 - \frac{0.25 \cdot orgC}{orgC + \exp(3.72 - 2.95 \cdot orgC)} \quad (6)$$

$$f_{\text{hisand}} = 1 - \frac{0.7 \cdot (1 - \frac{m_s}{100})}{(1 - \frac{m_s}{100}) + \exp[-5.51 + 22.9 \cdot (1 - \frac{m_s}{100})]} \quad (7)$$

where m_s is the percent sand content (0.05–2.00 mm diameter particles), m_{silt} is the percent silt content (0.002–0.05 mm diameter particles), m_c is the percent clay content (<0.002 mm diameter particles), and $orgC$ is the percent organic carbon content of the layer (%).

In this study, the harmonized world soil database (HWSD) version 1.2 [31] was used as the input data to compute the K factor. HWSD is a 30 arc-second raster database with over 15,000 different soil mapping units that combines the existing regional and national database of global soil information (SOTER, ESD, Soil Map of China, WISE) with the information contained within the FAO-UNESCO Soil Map of the World (FAO, 1971–1981) (https://www.fao.org/soils-portal/data-hub/soil-maps-and-databases/harmonized-world-soil-database-v12/en/, accessed on 1 December 2022). The HWSD data were also resampled to 30 m in ArcGIS 10.2 software.

Topography plays a significant role in soil erosion, and steep terrain is more likely to cause severe soil erosion. The topographic factor (LS) represents the effects of slope length (L) and slope steepness (S) on the soil erosion. Combining L and S factors can provide an efficient method to calculate soil erosion. In this study, the LS factor was computed using Equation (8), given by Wischmeier et al. [12] and Renard et al. [13].

$$\mathrm{LS} = \left(\frac{\lambda}{22.1}\right)^{m} \times (65.41 \times \sin^2\theta + 4.56 \times \sin\theta + 0.065) \quad (8)$$

where, λ is slope length in meter, θ is the angle of the slope, and m is 0.2 for slopes less than 1%, 0.3 for 1–3.5%, 0.4 for 3.5–5%, and 0.5 for slopes more than 5%.

The LS factor was calculated with a digital elevation model (DEM) generated from Advanced Spaceborne Thermal Emission and Reflection Radiometer (ASTER) Global Digital Elevation Model Version 2 (GDEM V2) data (https://asterweb.jpl.nasa.gov/gdem.asp, accessed on 1 December 2022). The ASTER GDEM V2 includes 30 m resolution images in GeoTIFF format.

The crop management factor (C) is defined as the potential soil loss under different land use/land cover and during crop rotations, construction, or other management activities [12,13]. The C factor is the ratio of soil loss from land cropped under specific conditions to corresponding loss from clean-tilled, continuous fallow [12]. Of the various methods used to calculate the C factor, RS data and GIS technique have been widely used due to their spatial and temporal advantages. The normalized difference vegetation index (NDVI), an indicator of vegetation cover, was used to compute the C factor, using Equation (9), as given by Knijff et al. [32]:

$$\mathrm{C} = \exp\left(-\alpha \cdot \frac{\mathrm{NDVI}}{\beta - \mathrm{NDVI}}\right) \quad (9)$$

where α and β are the parameters that determine the shape of the curve relating to NDVI and the C factor. The α value of 2 and β value of 1 provide better results [32]. NDVI images has 30-m resolution.

The conservation support practice factor (P) is the soil loss ratio with a specific support practice to the corresponding loss with upslope and downslope tillage [12,13]. It represents the effects of practices such as contouring, strip cropping, and terracing, and it is an important factor in controlling soil erosion. The values of the P factor range from 0 to 1, and they were calculated according to the cultivating methods and slope proposed by Shin [33]. In the study, contouring was selected as the cultivating method for HTYZ, and the value of P factor could be assigned based on the different slope ranges and contouring (Table S1). In HTYZ, a value approaching 0 indicates good conservation practice, and a value approaching 1 indicates poor conservation practice.

2.3. Mapping the Siltation Area Change of Lake Ulansuhai

The visual interpretation of RS images is a common method for calculating change in an area. It is widely used due to its high accuracy. In this study, Landsat satellite (Landsat TM and OIL) multi-spectral images with 30 m resolution were acquired to compute the change in the siltation area. The images from post-annual flood season (June to September) were downloaded from the United States Geological Survey (USGS) website (https://landsatlook.usgs.gov, accessed on 1 December 2022). Due to the cloud occlusion, the images from 1988, 1990, and 2012 were selected from April of the following year (before the

flood season). In order to better distinguish the difference between siltation land and other land use types, the images were enhanced before visual interpretation, including using standard false color images and histogram equalization. The goal of image enhancement was to improve the visual interpretability of an image by increasing the apparent distinction between features [34]. Geometric correction is important for multi-temporal images, which can accurately demonstrate the change in land use types. Geometrically corrected images were used to map the siltation of Lake Ulansuhai caused by HTYZ soil erosion from 1986 to 2015 using image enhancement and visual interpretation methods.

3. Results

3.1. The Applicability of CHELSA Precipitation Data

In this study, CHELSA precipitation data were used to calculate rain erosivity and assess the soil erosion in a small watershed using the RUSLE model. However, the applicability of the CHELSA precipitation data in HTYZ needs to be verified. In order to verify the applicability of the data, rainfall data from 1986 to 2005 at nine gauged stations situated around HTYZ were collected (Figure S1), and the mean annual precipitation of gauged stations and CHELSA precipitation data for the past 20 years was calculated. The result showed that the CHELSA precipitation data has strong correlation with the gauged stations precipitation data (R^2 = 0.8959) (Figure 2), indicating CHELSA precipitation data could be used with high accuracy in the HTYZ. Therefore, CHELSA precipitation data was used as the precipitation data for the RUSLE, and the result also suggests that the data could overcome the limitation of a lack of gauged stations and help in an accurate assessment of soil erosion in areas with ungauged station.

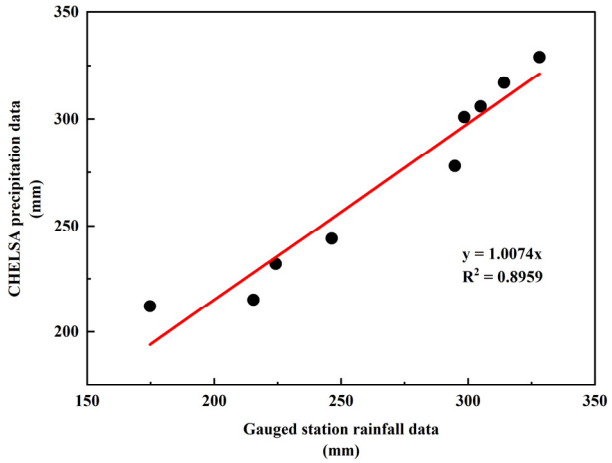

Figure 2. Relationship between the CHELSA precipitation data with gauged station rainfall data.

3.2. Estimation of RUSLE Parameters and Mean Annual Soil Erosion

3.2.1. Rainfall Erosivity Factor (R)

In the study, the mean annual rainfall during 30 years in HTYZ ranges from 204 to 360 mm, and rainfall data shows a trend of increasing from northeast to south. The southern part is the rainfall center of both HTYZ and the Ulansuhai east watershed (Figure S1). The R factor in the HTYZ ranged from 106.528 to 194.2 MJ mm ha^{-1} h^{-1} yr^{-1} (Figure 3a), and it showed a decreasing trend from south to north, reaching the highest value in the southern mountainous area and the lowest value in the northwestern parts of the region. It suggests that the southern mountainous area is subjected to a highly aggressive climate.

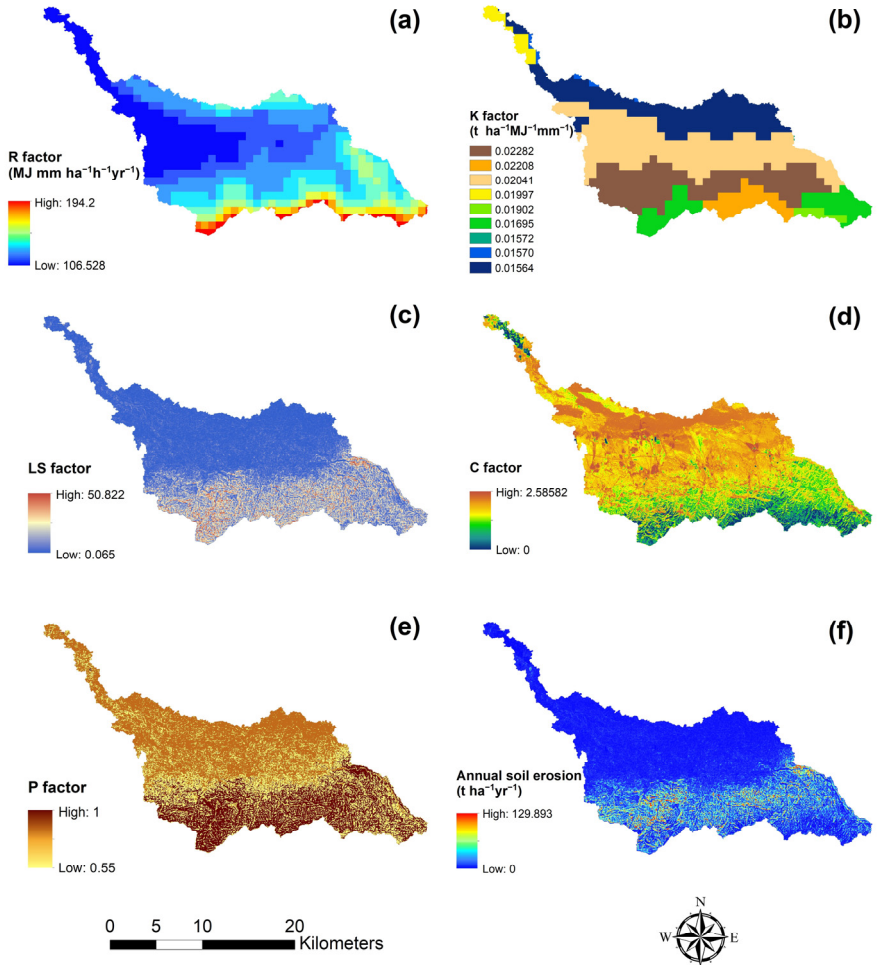

Figure 3. Parameters of calculated RUSLE, and the annual soil erosion of HTYZ area. Specifically, (**a**) R factor, (**b**) K factor, (**c**) LS factor, (**d**) C factor, (**e**) P factor, and (**f**) soil annual loss of HTYZ area, respectively.

3.2.2. Soil Erodibility Factor (K)

The K factor in HTYZ was calculated from the soil map in order to generate the soil erodibility map, and the low value of the K factor represents high resistance to erosion. In this study, there are nine soil types in the HTYZ area, and the value of the K factor ranged from 0.01564 to 0.02282 t ha^{-1} MJ^{-1} mm^{-1} (Figure 3b). The maximum value of 0.02282 represents Calcaric Cambisols, a type of soil that is derived in alluvial, colluvial, and aeolian deposits, and is a common soil type in the erosion area. Calcaric Cambisols occupied 23.65% of the HTYZ region (Table S2), and mainly occupied the southern mountainous area. Moreover, the K map showed that it had a low erosion resistance in the central and southern areas and had a low erosion resistance in northern parts of HTYZ. However, the area closer to Lake Ulansuhai also has a relatively low erosion resistance.

3.2.3. Topographic Factor (LS)

The LS value represents the effect of terrain on soil erosion, and the LS factor in HTYZ ranged from 0.065 to 50.822 (Figure 3c). In this study, the LS factor with a value of less than 1 occupied 33.11% of HTYZ and was mostly distributed in the northern and central part of HTYZ. The LS values of half of the area of HTYZ ranged from 1 to 15, indicating that most of the area has a relatively flat terrain. Moreover, LS values of more than 30 only occupied 0.83% of this area, mainly distributing in southern mountainous region (Table S3).

3.2.4. Crop Management Factor (C)

The C factor in HTYZ ranged from 0 to 2.58582 (Figure 3d). Most of the area of HTYZ had a relatively high C factor value, where a value of more than 5 accounted for about 80% the area. It indicates that low vegetation coverage is an important characteristic of semi-arid regions (Table S4). However, the southern mountainous area had a relatively low C value due to steep terrain.

3.2.5. Conservation Support Practice Factor (P)

The P factor represents the measures to reduce soil erosion. The P factor was calculated based on the terrain data. The result was classified by slope difference. In this study, the P factor in HTYZ ranged from 0.55 to 1 (Figure 3e). A P factor value of 0.8 accounted for about half of the area of HTYZ, indicating that most of HYTZ has a relatively flat terrain. Moreover, the value of 1 occupied 14.91% of the area of HTYZ, and it also suggests that the southern part of HTYZ had little conservation practices (Table S5).

3.2.6. Estimation of Mean Annual Soil Erosion

By using the RUSLE model with multi-source RS data, the mean annual soil loss of the HTYZ area during 1986 to 2015 was estimated. The result showed that soil loss in HTYZ ranged from 0 to 129.893 t ha^{-1} yr^{-1} (Figure 3f) with an average soil erosion for the entire area of 6.45 t ha^{-1} yr^{-1}. It showed that the soil erosion area with more than 25 t ha^{-1} yr^{-1} was mainly distributed in the southern mountainous area, and it was the accumulative result of high rainfall, vulnerable erosion soil type, and steep terrain. The northern and central parts had low soil loss, with the average soil loss less than 6.45 t ha^{-1} yr^{-1}.

3.3. Assessment of the Severity Level of Soil Erosion

According to the standard for classification and gradation of soil erosion (SL 190-2007) set by the Ministry of Water Resources of China, five categories of erosion severity class (t ha^{-1} yr^{-1}) are delineated: very slight (0–10), slight (10–25), moderate (25–50), severe (50-80), and extreme severe (80-150) (Figure 4). The area with very slight erosion severity occupied 80.06% of HTYZ and was generally distributed in the northern and central areas. The area with extreme severity of erosion occupied 0.06% of HTYZ and was distributed in the southern mountainous area, which has the presence of steep slopes, high rainfall, and erodible soil types. Other classes such as light, moderate, and severe accounted for 13.18%, 5.78%, and 0.92% of the total area, respectively (Table S6).

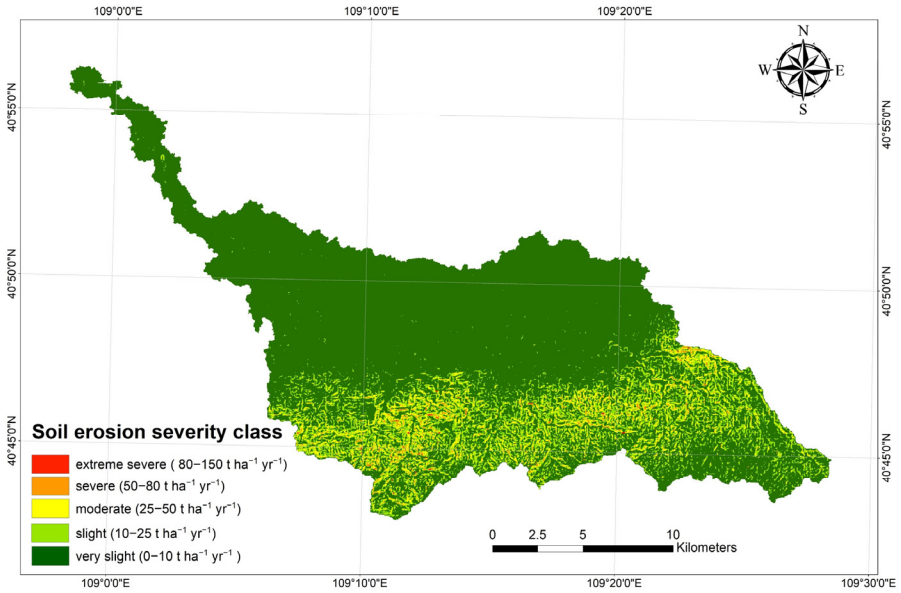

Figure 4. Soil erosion severity level of HTYZ.

3.4. Lake Ulansuhai Siltation Area

Based on the Landsat TM and OLI satellite images, the siltation area of Lake Ulansuhai caused by the soil erosion of HTYZ was estimated through the visual interpretation method. The result showed the siltation area had a large change during the past 30 years (Figure 5). The total siltation area was 223.83 ha with an annual average of 7.46 ha/yr. Moreover, significant siltation in Lake Ulansuhai (96.35 ha) was caused by the soil erosion in 1990, and the soil erosion in 1997 and 2013 caused relatively big amounts of siltation with 28.93 ha and 51.48 ha, respectively. Furthermore, the result showed that Lake Ulansuhai was affected by soil erosion in the HTYZ area every year, but it has different siltation directions due to changes of river the during the past 30 years.

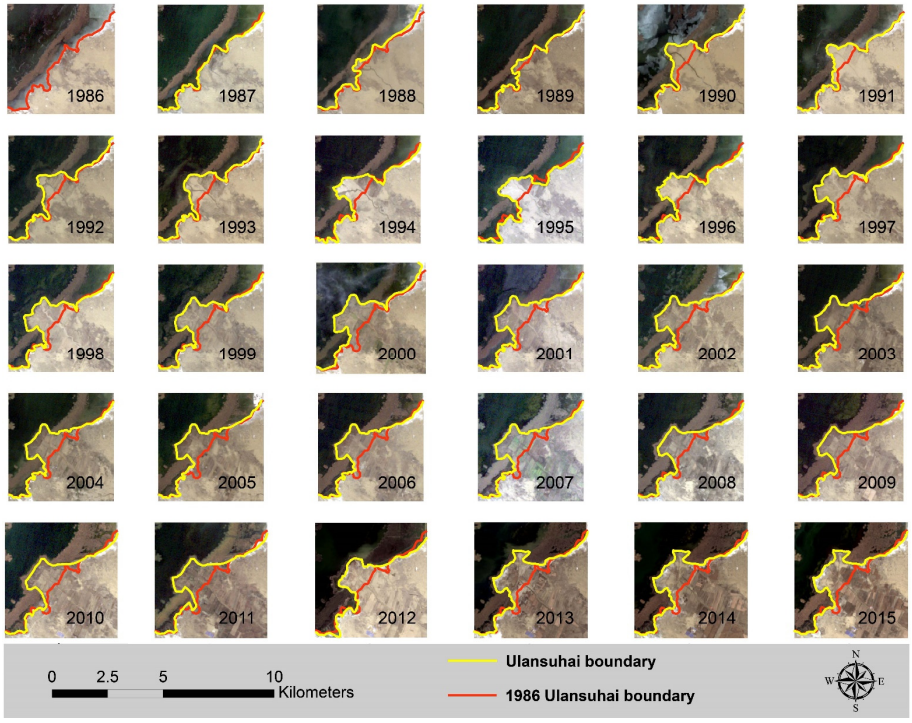

Figure 5. Annual changes of Lake Ulansuhai boundaries, partly due to siltation caused by soil erosion in the HTYZ area.

3.5. The Effect of Floods on Soil Erosion during Flood Season

In order to better understand the impact of floods during the flood season on the changes in siltation areas of lakes in arid regions, the change trend between mean annual precipitation and flood season precipitation was plotted for the change in the siltation area of Lake Ulansuhai, using the CHELSA precipitation data (Figure 6). The result showed that the rainfall during the flood reason accounted for 70% to 90% of the annual rainfall in most years. The change in siltation was similar to the trend of rainfall. The increase in the siltation area in 1990 and 1997 was due to the transient rainstorms, and the decrease of the siltation area in 2008 and 2012 was due to the increase in water levels caused by continuous rainfall. As the lake water level was controlled (the water level of Lake Ulansuhai is controlled at 1085 m above mean sea level) and there was a decrease in rainfall, the siltation area increased rapidly in 2010 and 2013. It suggests that the rainfall in flood seasons plays an important role in soil erosion and the siltation of the lake.

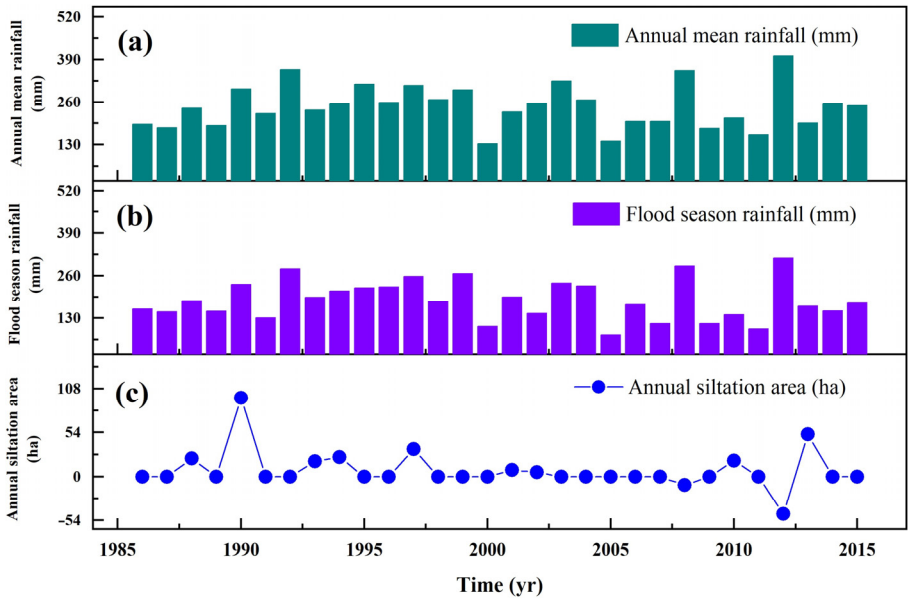

Figure 6. Annual trend of (**a**) annual mean rainfall, (**b**) flood season rainfall, and (**c**) annual siltation, respectively, from 1986 to 2015.

4. Discussion

4.1. The Factors Effecting Soil Erosion in a Small Watershed of a Semi-Arid Region

Soil erosion could be affected by precipitation, land use, terrain, soil type, etc. Many studies have estimated soil erosion using the RUSLE model because of its simplicity and effectiveness. The R factor has been proven to be the most highly correlated factor to soil erosion globally [12,35–38]. As a small watershed in a semi-arid region, the value of the R factor in HTYZ ranged from 106.528 to 194.2 MJ mm ha^{-1} h^{-1} yr^{-1}. The result is less than the study of Zhuang et al. [39] estimated for soil erosion of China in 2018. We think that the difference in the results of the two studies is the time selection. In this study, the R factor is calculated using a long time period, rather than using data that of a single year. Compared with other ecosystems, the maximum R factor in wet regions, such as southern India, is usually more than 1000 MJ mm ha^{-1} h^{-1} yr^{-1} [16,40,41]. However, the value of the R factor in semi-arid and arid regions, such as Ethiopia, Algeria, Arabia, and northwest China, is significantly less than wet area values due to low rainfall. Farhan et al. [42] and Djoukbala et al. [18] assessed soil erosion in semi-arid and arid regions, and found that the value of the R factor ranged from dozens to hundreds MJ mm ha^{-1} h^{-1} yr^{-1}. The study of Woldemariam et al. [43] shows that the R factor in Ethiopia's Gobele watershed ranges from 200 to 900 MJ mm ha^{-1} h^{-1} yr^{-1}, but it plays an important role in soil erosion. The study of Alsafadi et al. [44] shows that increased soil erosion caused by the R factor accounted for 34.65%. In the HTYZ area, the soil loss is also located in the range. In China, the study of Wu et al. [45] shows that the R factor is the key factor in the Three Rivers Headwaters Region. The study of Wang et al. [46] also shows that the R factor contributed more than the C factor in northern China. In this study, we suggest that the R factor is one of the key factors in estimating the soil erosion in small watersheds of semi-arid regions.

In comparison of wet areas, land cover type is also one of the main factors of soil erosion in the semi-arid area because the land could not be protected by vegetation. The study of Rao et al. [47] suggests that the C factor was a more sensitive driver than the R factor for soil erosion. The study of Golijanin et al. [48] suggests that increasing vegetation cover could decrease soil erosion. The study of Alsafadi et al. [44] shows that C is the key factor followed by the R factor in soil erosion, and the decrease in soil erosion is in part caused by an increase in the C factor (36.82%). The study of Teshome et al. [49] also suggests that land cover change plays a key role in decreasing soil erosion in the Muger sub-basin in Ethiopia. Due to the different types of land cover, the value of the C factor is

different for the semi-arid, arid, and wet regions. In wet regions, the land is mainly covered by forest, and the value of the C factor is less than 0.1 [16,40,50]. However, the semi-arid and arid regions are mainly covered by grassland, sand, and bare land with the value of C more than 0.5 [18]. HTYZ is mainly covered by grassland and sand, and the value of the C factor exceeding 0.5 for more than half of the area of HTYZ. It also suggests that the C factor is an important factor in the soil loss in the area. Furthermore, we think that the C factor is a key factor in decreasing soil erosion. The study of Wang et al. [46] showed that vegetation greening has partly offset water erosion risk in China in past decades, and the study of Wang et al. [51] also shows that the change of land cover could effectively control soil erosion in small watersheds in the Loess Plateau of China. Thus, we suggest that proper measurement needs to be considered in increasing vegetation to decrease soil erosion in semi-arid regions.

Another factor, terrain, is also one of the factors sensitive to soil erosion [52]. Increasing of slope may increase the soil erosion because it increases the movement of sediment. The study of Zhu et al. [53] suggests that increasing soil erosion with an increase in the slope causes large organic carbon loss. In this study, the mountain area, the southern part of HTYZ, is an important area for soil erosion. Due to the low vegetation coverage and concentrated rainfall, more attention needs to be paid to the mountain and steep area for decreasing soil erosion in this semi-arid region.

4.2. The Applicability of CHELSA Precipitation Data in a Small Watershed in a Semi-Arid Region

Rainfall is a vital factor in calculating soil erosion. The calculation of rainfall erosivity needs data from many gauged stations to ensure the accuracy of the R factor, and several studies have calculated rainfall erosion using the interpolation method. However, previous studies have mainly been conducted in large regions and areas that have gauge stations. Feng et al. [31] calculated the rainfall erosivity in the Loess Plateau in China using data from more than 50 gauged stations, while Du et al. [17] used more than 20 gauged stations' data to calculate the soil loss in northwest China. For a small study area of 300 km^2, Thomas et al. [16] also used nine gauged station data to assess soil erosion. Due to the scarcity of gauged stations in many of the arid regions, rainfall data cannot be used to calculate erosion effectively by using interpolation [27], causing estimation of soil erosion for arid areas to be difficult. In this study, CHELSA was used to calculate the R factor and had a strong correlation with gauge station data around the HTYZ area, suggesting that soil erosion could be estimated in small watersheds. Compared with other satellite precipitation data, CHELSA data could provide the data for long time periods on a monthly timescale. Although the data may also cause uncertainty by not including the rainfall intensity, the data could provide a reference for the small ungauged areas in semi-arid regions during a long time period.

4.3. The Effect of Floods on Soil Erosion in Semi-Arid Region

Floods is an important factor for soil erosion and sediment transport, and they could increase the soil sediment by increasing river discharge [54]. In a semi-arid area, floods can cause serious impact due to the fragile ecological environment of arid regions. In this study, a flood during flood season plays an important role in soil loss, and the sediment enters the lake through the high river discharge during the flood period. It caused the large siltation of Lake Ulansuhai after the flood years. In other areas, the studies of both Piacentini et al. [55] and Wang et al. [56] show that a single flood event had a significant effect on sediment delivery in the Loess Plateau of China, and rainfall and runoff were main driving factors for soil erosion and sediment transport. The study of Zheng et al. [57] also showed that a large flood event had an important contribution to sediment transport. The study of Qiankun et al. [58] suggests that a flood event played an important role in increasing the soil loss in the Hengduan mountain region in southwest China. Moreover, the study of Xu et al. [59] suggests that floods should be considered in estimating soil erosion, because they may cause an uncertain R factor. In this study, the soil loss may be underestimated due

to the lack of rainfall intensity. In semi-arid areas, the study of Liu et al. [60] shows that sediment and particles organic carbon increased quickly, caused by soil erosion during an episodic flood event in a semi-arid grassland area. Compared with other studies, we think that floods may increase the risk of soil loss in the semi-arid areas because of the land cover. Thus, potential management must also be discussed from this perspective, as the study of Bhatti et al. [61] shows that settling reservoirs can reduce sediment entry in a river network, and the study of Mahoney et al. [62] suggests that the reestablishment of native trees and recreated surface microtopography could decrease the soil erosion of the watershed. The studies of both Yao et al. [63] and Zhang et al. [64] on the Loess Plateau suggest that silt dam measures and ecological construction of soil and water conservation projects have a good flood- and sand-reduction effect on small- and medium-intensity rainfalls. Thus, we suggest that flood events in the semi-arid region examined in the present study may increase the risk of siltation of the Lake Ulansuhai, and the reasonable measures, such as building settling reservoirs, etc., need to be conducted to decrease the risk of siltation of the lake.

5. Conclusions

Making up a classical soil erosion district in the semi-arid and arid region, the soil erosion in HTYZ from 1986 to 2015 (30 years) was estimated. The soil loss in HTYZ ranged from 0 to 129.893 t ha^{-1} yr^{-1} with an average soil erosion for the entire area of 6.45 t ha^{-1} yr^{-1}. Moreover, the results showed that 80.06% of the total HTYZ area is affected by very slight soil erosion, and severe soil erosion area accounted for less than 1%. The southern part of HTYZ is the area with the most extreme soil erosion, and the northern and central parts of HTYZ had relatively light soil erosion. As the first application of CHELSA precipitation data in a small watershed of a semi-arid region, we verified the applicability of the data. The results showed that the CHELSA data strongly correlated with gauged station precipitation data, with R^2 at 0.8959. Furthermore, our result suggested that floods during the flood season were the main driving factor of soil erosion in the small watershed of HTYZ, and the siltation of Lake Ulansuhai caused by HTYZ soil erosion reached 228.83 ha. Moreover, further work needs to focus on the estimation and impact of the R factor, as well as the impact and contribution of floods during the flood season to the soil erosion and lake siltation, by using multi-source RS and in-situ data. Soil loss is mainly transferred by river and then enters into the lake; thus, the amount of material carried by the river and the connectivity of the slope and river/lake system also need more quantitative studies in further work. The study could provide a reference to assess soil erosion in a small watershed of a semi-arid region and to protect the fragile ecology of the area.

Supplementary Materials: The following supporting information can be downloaded at: https://www.mdpi.com/article/10.3390/land12020440/s1.

Author Contributions: Z.Z.: methodology, validation, writing—original draft preparation R.Y.: conceptualization, writing—review and editing, supervision, funding acquisition. All authors have read and agreed to the published version of the manuscript.

Funding: This research was funded by the National Natural Science Foundation of China (Grant Nos. 52279067 and 51869014), National Key Research and Development Program of China (Grant No. 2021YFC3201203), Major Science and Technology Projects of Inner Mongolia Autonomous Region (Grant Nos. 2020ZD0009), and Open Project Program of the Ministry of Education Key Laboratory of Ecology and Resources Use of the Mongolian Plateau (Grant No. KF2020006), and Project of Key Laboratory of River and Lake in Inner Mongolia Autonomous Region.

Data Availability Statement: Not applicable.

Acknowledgments: We thank our colleagues at the Inner Mongolia Key Laboratory of River and Lake Ecology for their help.

Conflicts of Interest: The authors declare no conflict of interest.

References

1. Montgomery, D.R. Soil erosion and agricultural sustainability. *Proc. Natl. Acad. Sci. USA* **2007**, *104*, 13268. [CrossRef] [PubMed]
2. Lal, R. Soil erosion and the global carbon budget. *Environ. Int.* **2003**, *29*, 437–450. [CrossRef] [PubMed]
3. Wynants, M.; Solomon, H.; Ndakidemi, P.; Blake, W.H. Pinpointing areas of increased soil erosion risk following land cover change in the Lake Manyara catchment, Tanzania. *Int. J. Appl. Earth Obs. Geoinf.* **2018**, *71*, 1–8. [CrossRef]
4. García-Ruiz, J.M.; Beguería, S.; Lana-Renault, N.; Nadal-Romero, E.; Cerdà, A. Ongoing and Emerging Questions in Water Erosion Studies. *Land Degrad. Dev.* **2017**, *28*, 5–21. [CrossRef]
5. Alatorre, L.C.; Beguería, S.; García-Ruiz, J.M. Regional scale modeling of hillslope sediment delivery: A case study in the Barasona Reservoir watershed (Spain) using WATEM/SEDEM. *J. Hydrol.* **2010**, *391*, 109–123. [CrossRef]
6. Stefanidis, S.; Alexandridis, V.; Ghosal, K. Assessment of Water-Induced Soil Erosion as a Threat to Natura 2000 Protected Areas in Crete Island, Greece. *Sustainability* **2022**, *14*, 2738. [CrossRef]
7. Köninger, J.; Panagos, P.; Jones, A.; Briones, M.J.I.; Orgiazzi, A. In defence of soil biodiversity: Towards an inclusive protection in the European Union. *Biol. Conserv.* **2022**, *268*, 109475. [CrossRef]
8. Cerdan, O.; Govers, G.; Le Bissonnais, Y.; Van Oost, K.; Poesen, J.; Saby, N.; Gobin, A.; Vacca, A.; Quinton, J.; Auerswald, K.; et al. Rates and spatial variations of soil erosion in Europe: A study based on erosion plot data. *Geomorphology* **2010**, *122*, 167–177. [CrossRef]
9. Kinnell, P.I.A. A review of the design and operation of runoff and soil loss plots. *CATENA* **2016**, *145*, 257–265. [CrossRef]
10. Nearing, M.A.; Foster, G.R.; Lane, L.J.; Finkner, S.C. A process-based soil erosion model for USDA-water erosion prediction project technology. *Trans. ASAE* **1989**, *32*, 1587–1593. [CrossRef]
11. Morgan, R.P.C.; Quinton, J.N.; Smith, R.E.; Govers, G.; Poesen, J.W.A.; Auerswald, K.; Chisci, G.; Torri, D.; Styczen, M.E. The European Soil Erosion Model (EUROSEM): A dynamic approach for predicting sediment transport from fields and small catchments. *Earth Surf. Process. Landf.* **1998**, *23*, 527–544. [CrossRef]
12. Wischmeier, W.H.; Smith, D.D. *Predicting rainfall erosion losses—A guide to conservation planning*; USDA, Science and Education Administration: Hyattsville, Maryland, 1978.
13. Renard, K.G.; Foster, G.R.; Weesies, G.A.; McCool, D.K.; Yoder, D.C. *Predicting soil erosion by water: A guide to conservation planning with the Revised Universal Soil Loss Equation (RUSLE)*; U.S. Department of Agriculture: Washington, DC, USA, 1997.
14. Arnold, J.G.; Srinivasan, R.; Muttiah, R.S.; Williams, J.R. Large area hydrologic modeling and assessment part i: Model development1. *JAWRA J. Am. Water Resour. Assoc.* **1998**, *34*, 73–89. [CrossRef]
15. Markose, V.J.; Jayappa, K.S. Soil loss estimation and prioritization of sub-watersheds of Kali River basin, Karnataka, India, using RUSLE and GIS. *Environ. Monit. Assess.* **2016**, *188*, 225. [CrossRef]
16. Thomas, J.; Joseph, S.; Thrivikramji, K.P. Assessment of soil erosion in a tropical mountain river basin of the southern Western Ghats, India using RUSLE and GIS. *Geosci. Front.* **2018**, *9*, 893–906. [CrossRef]
17. Du, H.Q.; Dou, S.T.; Deng, X.H.; Xue, X.; Wang, T. Assessment of wind and water erosion risk in the watershed of the Ningxia-Inner Mongolia Reach of the Yellow River, China. *Ecol. Indic.* **2016**, *67*, 117–131. [CrossRef]
18. Djoukbala, O.; Mazour, M.; Hasbaia, M.; Benselama, O. Estimating of water erosion in semiarid regions using RUSLE equation under GIS environment. *Environ. Earth Sci.* **2018**, *77*, 345. [CrossRef]
19. Bezak, N.; Ballabio, C.; Mikoš, M.; Petan, S.; Borrelli, P.; Panagos, P. Reconstruction of past rainfall erosivity and trend detection based on the REDES database and reanalysis rainfall. *J. Hydrol.* **2020**, *590*, 125372. [CrossRef]
20. Moradi, H.; Oldeland, J. Climatic stress drives plant functional diversity in the Alborz Mountains, Iran. *Ecol. Res.* **2019**, *34*, 171–181. [CrossRef]
21. Zuquim, G.; Costa, F.R.C.; Tuomisto, H.; Moulatlet, G.M.; Figueiredo, F.O.G. The importance of soils in predicting the future of plant habitat suitability in a tropical forest. *Plant Soil* **2019**, *450*, 151–170. [CrossRef]
22. Fang, L.Q.; Tao, S.L.; Zhu, J.L.; Liu, Y. Impacts of climate change and irrigation on lakes in arid northwest China. *J. Arid. Environ.* **2018**, *154*, 34–39. [CrossRef]
23. Kazamias, A.P.; Sapountzis, M. Spatial and temporal assessment of potential soil erosion over Greece. In Proceedings of the 10th World Congress of the European Water Resources Association (EWRA) on Water Resources and Environment (EWRA2017), Athens, Greece, 5–9 July 2017; pp. 315–321.
24. Chen, Q.; Yu, R.H.; Hao, Y.L.; Wu, L.H.; Zhang, W.X.; Zhang, Q.; Bu, X.N. A New Method for Mapping Aquatic Vegetation Especially Underwater Vegetation in Lake Ulansuhai Using GF-1 Satellite Data. *Remote Sens.* **2018**, *10*, 1279. [CrossRef]
25. Yu, R.H.; Li, C.Y.; Liu, T.X.; Xu, Y.P. Change of Wetland Environment in Wuliangsuhai. *Acta Geogr. Sin.* **2004**, *59*, 948–955. [CrossRef]
26. Hurni, H. Erosion-Productivity-Conservation Systems in Ethiopia. In Proceedings of the 4th International Conference on Soil Conservation, Maracay, Venezuela, 3–9 November 1985; pp. 654–674. [CrossRef]
27. Karger, D.N.; Conrad, O.; Böhner, J.; Kawohl, T.; Kreft, H.; Soria-Auza, R.W.; Zimmermann, N.E.; Linder, H.P.; Kessler, M. Climatologies at high resolution for the earth's land surface areas. *Sci. Data* **2017**, *4*, 170122. [CrossRef]
28. Shabani, F.; Kumar, L.; Esmaeili, A. Improvement to the prediction of the USLE K factor. *Geomorphology* **2014**, *204*, 229–234. [CrossRef]
29. Millward, A.A.; Mersey, J.E. Adapting the RUSLE to model soil erosion potential in a mountainous tropical watershed. *CATENA* **1999**, *38*, 109–129. [CrossRef]

30. Neitsch, S.L.; Arnold, J.G.; Kiniry, J.R.; Williams, J.R. *Soil and Water Assessment Tool Theoretical Documentation Version 2009*; Texas Water Resources Institute: College Station, TX, USA, 2011.
31. Feng, X.M.; Wang, Y.F.; Chen, L.D.; Fu, B.J.; Bai, G.S. Modeling soil erosion and its response to land-use change in hilly catchments of the Chinese Loess Plateau. *Geomorphology* **2010**, *118*, 239–248. [CrossRef]
32. Knijff, J.M.v.d.; Jones, R.J.A.; Montanarella, L. *Soil erosion risk: Assessment in Europe: European Soil Bureau*; European Commission: Brussels, Belgium, 2000.
33. Shin, G.J. *The Analysis of Soil Erosion Analysis in Watershed Using GIS*; Gang-Won National University: Chuncheon, Republic of Korea, 1999.
34. Shalaby, A.; Tateishi, R. Remote sensing and GIS for mapping and monitoring land cover and land-use changes in the Northwestern coastal zone of Egypt. *Appl. Geogr.* **2007**, *27*, 28–41. [CrossRef]
35. Wischmeier, W.H. A Rainfall Erosion Index for a Universal Soil-Loss Equation1. *Soil Sci. Soc. Am. J.* **1959**, *23*, 246–249. [CrossRef]
36. Stocking, M.A.; Elwell, H.A. Prediction of subtropical storm soil losses from field plot studies. *Agric. Meteorol.* **1973**, *12*, 193–201. [CrossRef]
37. Lo, A.; El-Swaify, S.A.; Dangler, E.W.; Shinshiro, L. Effectiveness of El30 as an erosivity index in Hawaii. *Univ. Lanc.* **1985**.
38. Renard, K.G.; Freimund, J.R. Using monthly precipitation data to estimate the R-factor in the revised USLE. *J. Hydrol.* **1994**, *157*, 287–306. [CrossRef]
39. Zhuang, H.; Wang, Y.; Liu, H.; Wang, S.; Zhang, W.; Zhang, S.; Dai, Q. Large-Scale Soil Erosion Estimation Considering Vegetation Growth Cycle. *Land* **2021**, *10*, 473. [CrossRef]
40. Ganasri, B.P.; Ramesh, H. Assessment of soil erosion by RUSLE model using remote sensing and GIS—A case study of Nethravathi Basin. *Geosci. Front.* **2016**, *7*, 953–961. [CrossRef]
41. Biswas, S.S.; Pani, P. Estimation of soil erosion using RUSLE and GIS techniques: A case study of Barakar River basin, Jharkhand, India. *Model. Earth Syst. Environ.* **2015**, *1*, 42. [CrossRef]
42. Farhan, Y.; Nawaiseh, S. Spatial assessment of soil erosion risk using RUSLE and GIS techniques. *Environ. Earth Sci.* **2015**, *74*, 4649–4669. [CrossRef]
43. Woldemariam, G.; Iguala, A.; Tekalign, S.; Reddy, R. Spatial Modeling of Soil Erosion Risk and Its Implication for Conservation Planning: The Case of the Gobele Watershed, East Hararghe Zone, Ethiopia. *Land* **2018**, *7*, 25. [CrossRef]
44. Alsafadi, K.; Bi, S.; Abdo, H.G.; Al Sayah, M.J.; Ratonyi, T.; Harsanyi, E.; Mohammed, S. Spatial–temporal dynamic impact of changes in rainfall erosivity and vegetation coverage on soil erosion in the Eastern Mediterranean. *Environ. Sci. Pollut. Res.* **2022**. [CrossRef]
45. Wu, D.; Peng, R.; Huang, L.; Cao, W.; Huhe, T. Spatio-Temporal Analysis and Driving Factors of Soil Water Erosion in the Three-River Headwaters Region, China. *Water* **2022**, *14*, 4127. [CrossRef]
46. Wang, H.; Zhao, W.; Li, C.; Pereira, P. Vegetation greening partly offsets the water erosion risk in China from 1999 to 2018. *Geoderma* **2021**, *401*, 115319. [CrossRef]
47. Rao, W.; Shen, Z.; Duan, X. Spatiotemporal patterns and drivers of soil erosion in Yunnan, Southwest China: RULSE assessments for recent 30 years and future predictions based on CMIP6. *CATENA* **2023**, *220*, 106703. [CrossRef]
48. Golijanin, J.; Nikolić, G.; Valjarević, A.; Ivanović, R.; Tunguz, V.; Bojić, S.; Grmuša, M.; Lukić Tanović, M.; Perić, M.; Hrelja, E.; et al. Estimation of potential soil erosion reduction using GIS-based RUSLE under different land cover management models: A case study of Pale Municipality, B&H. *Front. Environ. Sci.* **2022**, *10*, 945789. [CrossRef]
49. Teshome, D.S.; Moisa, M.B.; Gemeda, D.O.; You, S. Effect of Land Use-Land Cover Change on Soil Erosion and Sediment Yield in Muger Sub-Basin, Upper Blue Nile Basin, Ethiopia. *Land* **2022**, *11*, 2173. [CrossRef]
50. Kayet, N.; Pathak, K.; Chakrabarty, A.; Sahoo, S. Evaluation of soil loss estimation using the RUSLE model and SCS-CN method in hillslope mining areas. *Int. Soil Water Conserv. Res.* **2018**, *6*, 31–42. [CrossRef]
51. Wang, J.; Lu, P.; Valente, D.; Petrosillo, I.; Babu, S.; Xu, S.; Li, C.; Huang, D.; Liu, M. Analysis of soil erosion characteristics in small watershed of the loess tableland Plateau of China. *Ecol. Indic.* **2022**, *137*, 108765. [CrossRef]
52. Bircher, P.; Liniger, H.P.; Prasuhn, V. Comparing different multiple flow algorithms to calculate RUSLE factors of slope length (L) and slope steepness (S) in Switzerland. *Geomorphology* **2019**, *346*, 106850. [CrossRef]
53. Zhu, Y.; Li, W.; Wang, D.; Wu, Z.; Shang, P. Spatial Pattern of Soil Erosion in Relation to Land Use Change in a Rolling Hilly Region of Northeast China. *Land* **2022**, *11*, 1253. [CrossRef]
54. Li, J.; Hao, Y.; Zhang, Z.; Li, Z.; Yu, R.; Sun, Y. Analyzing the distribution and variation of Suspended Particulate Matter (SPM) in the Yellow River Estuary (YRE) using Landsat 8 OLI. *Reg. Stud. Mar. Sci.* **2021**, *48*, 102064. [CrossRef]
55. Piacentini, T.; Galli, A.; Marsala, V.; Miccadei, E. Analysis of Soil Erosion Induced by Heavy Rainfall: A Case Study from the NE Abruzzo Hills Area in Central Italy. *Water* **2018**, *10*, 1314. [CrossRef]
56. Wang, L.L.; Yao, W.Y.; Tang, J.L.; Wang, W.L.; Hou, X.X. Identifying the driving factors of sediment delivery ratio on individual flood events in a long-term monitoring headwater basin. *J. Mt. Sci.* **2018**, *15*, 1825–1835. [CrossRef]
57. Zheng, M.G.; Liao, Y.S.; He, J.J. Sediment Delivery Ratio of Single Flood Events and the Influencing Factors in a Headwater Basin of the Chinese Loess Plateau. *PLoS ONE* **2014**, *9*, e112594. [CrossRef]
58. Qiankun, G.; Aijuan, W.; Wei, Q.; Zhijie, S.; Jiaguo, G.; Dandan, W.; Lin, D. Changes in the characteristics of flood discharge and sediment yield in a typical watershed in the Hengduan Mountain Region, Southwest China, under extreme precipitation events. *Ecol. Indic.* **2022**, *145*, 109600. [CrossRef]

59. Xu, Z.; Zhang, S.; Zhou, Y.; Hou, X.; Yang, X. Characteristics of watershed dynamic sediment delivery based on improved RUSLE model. *CATENA* **2022**, *219*, 106602. [CrossRef]
60. Liu, X.; Lu, X.; Yu, R.; Sun, H.; Li, Y.; Qi, Z.; Xue, H.; Zhang, Z.; Cao, Z.; Liu, T.; et al. Sediment and carbon dynamics during an episodic flood in an intermittent river. *Ecosphere* **2022**, *13*, e4248. [CrossRef]
61. Bhatti, M.T.; Ashraf, M.; Anwar, A.A. Soil Erosion and Sediment Load Management Strategies for Sustainable Irrigation in Arid Regions. *Sustainability* **2021**, *13*, 3547. [CrossRef]
62. Mahoney, D.; Blandford, B.; Fox, J. Coupling the probability of connectivity and RUSLE reveals pathways of sediment transport and soil loss rates for forest and reclaimed mine landscapes. *J. Hydrol.* **2021**, *594*, 125963. [CrossRef]
63. Yao, Z.; Yang, J.; Zhang, P.; Zhang, Y.; Liu, L.; Zhao, D. The Response Mechanisms of Topographic Changes in Small Loess Watershed under Rainstorm. *Sustainability* **2022**, *14*, 10472. [CrossRef]
64. Zhang, P.; Sun, W.; Xiao, P.; Yao, W.; Liu, G. Driving Factors of Heavy Rainfall Causing Flash Floods in the Middle Reaches of the Yellow River: A Case Study in the Wuding River Basin, China. *Sustainability* **2022**, *14*, 8004. [CrossRef]